
Thermal Re-Radiation Acceleration in the GNSS Orbit Modelling Based on Galileo Clock Parameters

Drazen Svehla¹

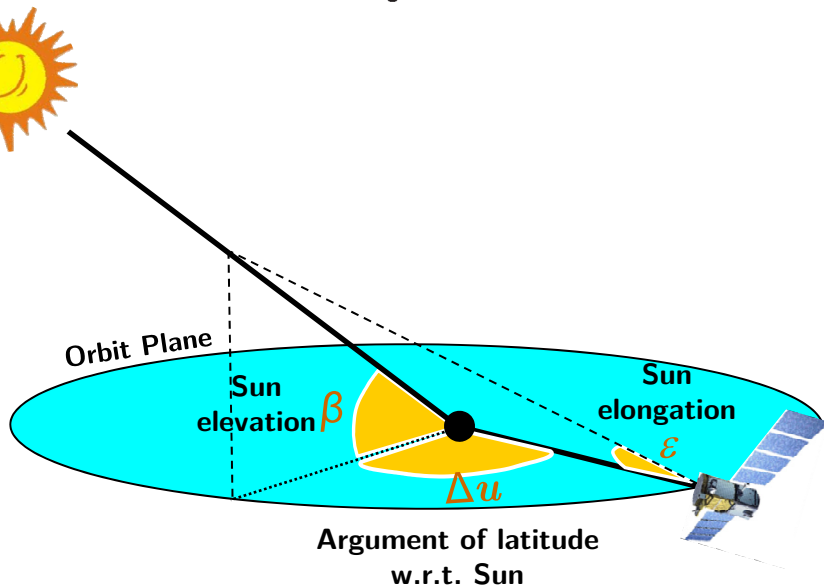
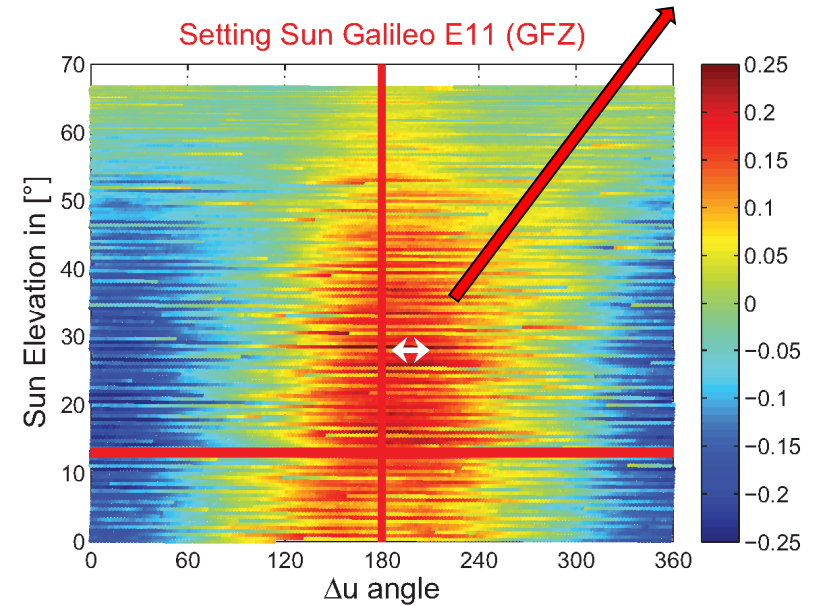
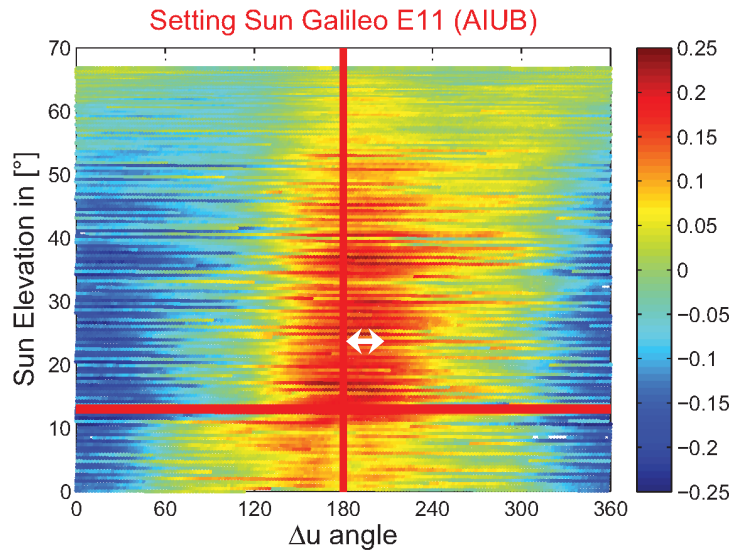
M. Rothacher¹, L. Cacciapuoti²

¹ETH Zurich, Institute of Geodesy and Photogrammetry, Switzerland

²ESA/ESTEC, Directorate of Science and Robotic Exploration, Noordwijk, Netherlands

Galileo Clock Parameters in the Sun-fixed Frame (daily time drift/bias removed)

Thermal inertia



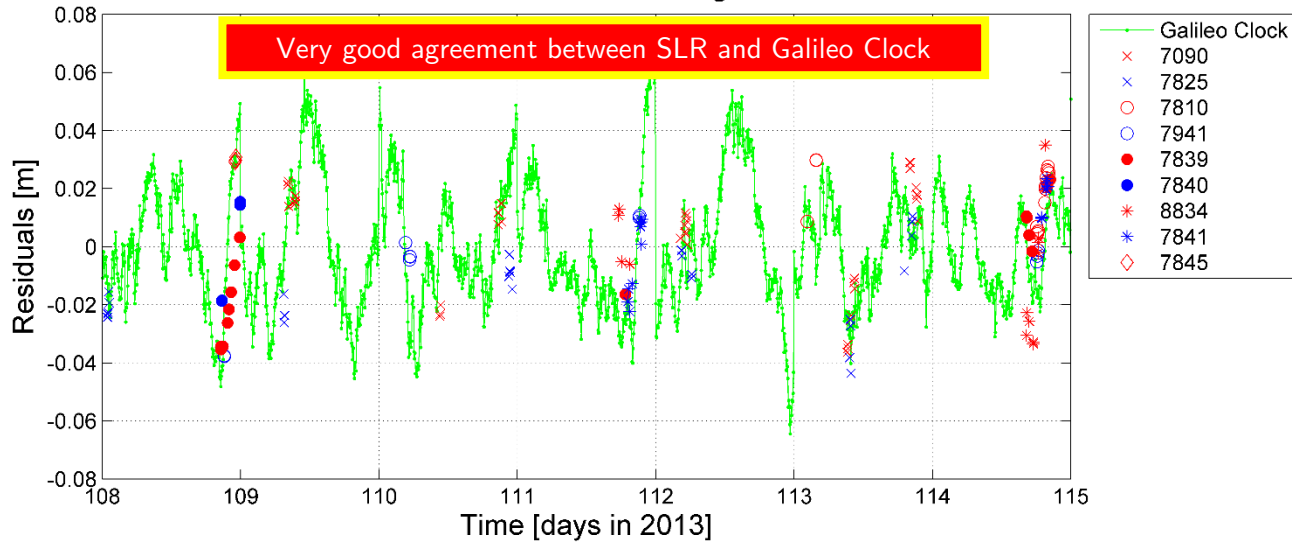
$$\Delta r = A \cdot \cos \beta \cos \Delta u$$



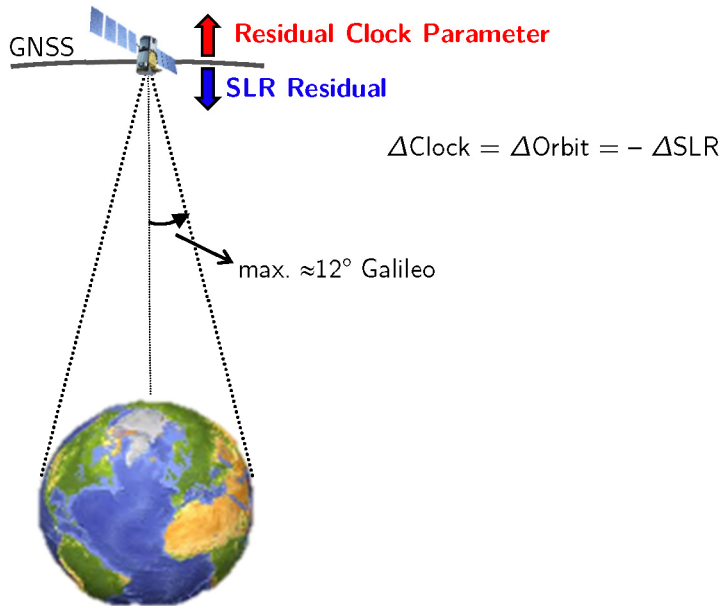
$$\delta_{clk} = \Delta r = -A \cdot \cos \varepsilon$$

Comparison of SLR and Galileo Clock

Galileo E11 Residual Clock Parameters Against SLR Residuals



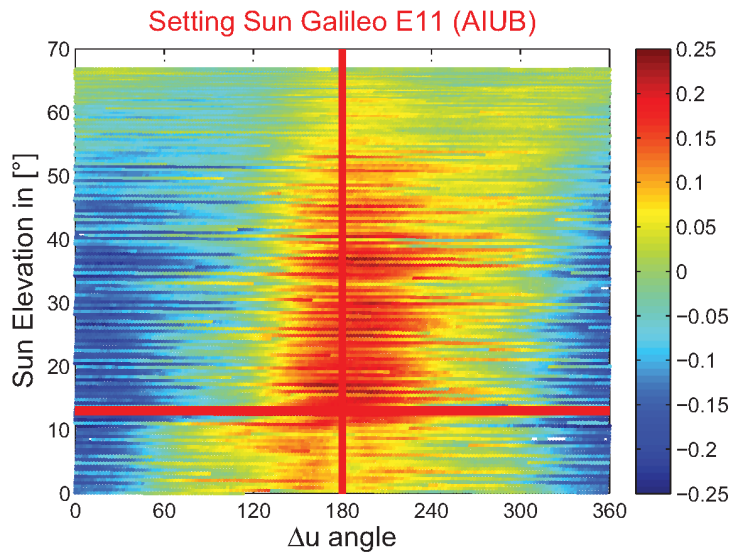
STD(MGEX CLOCK)=20.7 mm
 STD(Simulated CLOCK)=15.5 mm
 ↓
 STD(Orbit)=14 mm
 STD(SLR)=25.3 mm



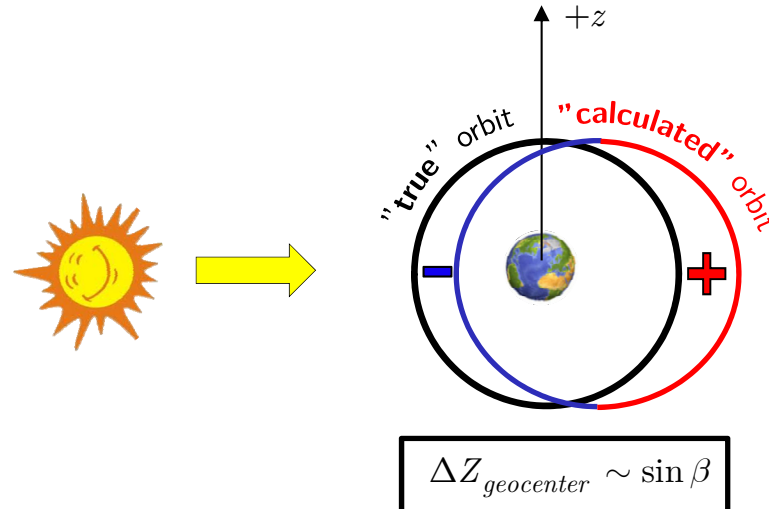
Galileo clock is showing smaller standard deviation compared to SLR! (MGEX and ground test)

Relation Between Clock, SLR Bias and Orbit Translation (geocenter)

Galileo Clock



Orbit Translation



$$\Delta r = A \cdot \cos \beta \cos \Delta u$$

$$\delta_{clk} = \Delta r = -A \cdot \cos \varepsilon$$



SLR Bias:

$$\bar{\delta}_{SLR} = \bar{\delta}_{const} + \frac{\sum n_i \cdot A \cos \varepsilon_i}{\sum n_i} = -2.4 \text{ cm} - 4.1 \text{ cm} = -6.5 \text{ cm}$$

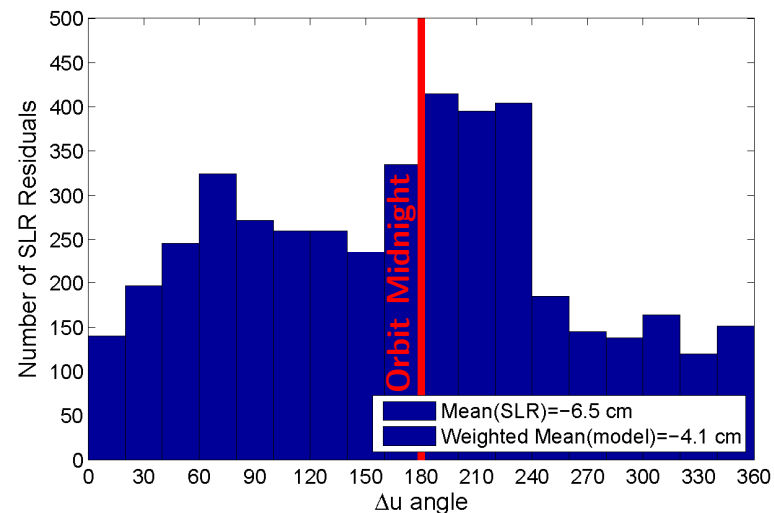
Observed
SLR Bias

$$-6.5 \text{ cm}$$



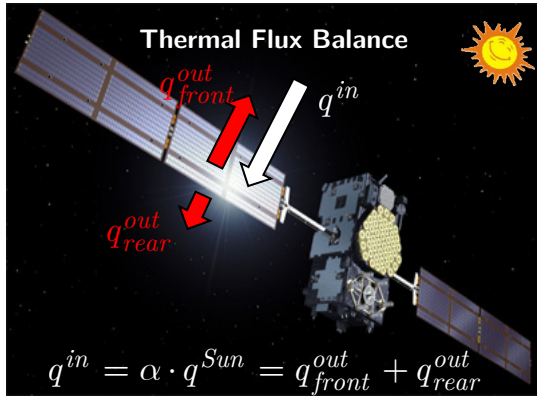
albedo? (wrong sign! increases the SLR bias)
antenna thrust? (wrong sign! increases the SLR bias)

SLR Residuals = "observed" - "calculated"

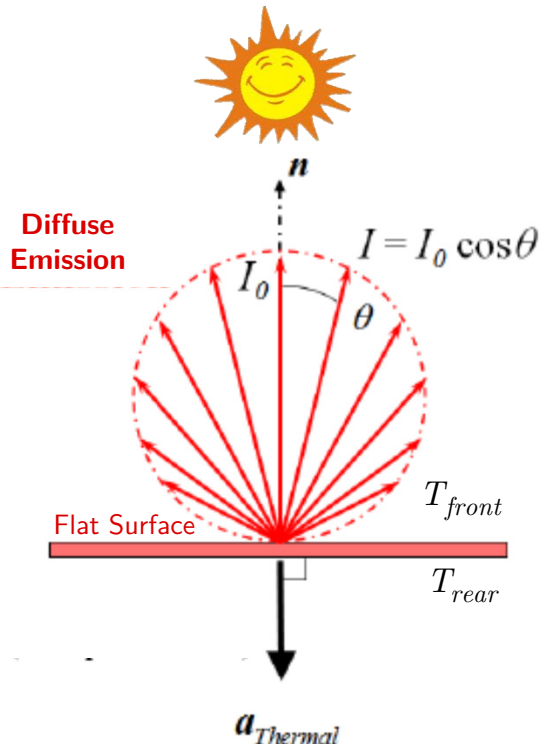


Thermal Re-Radiation Acceleration

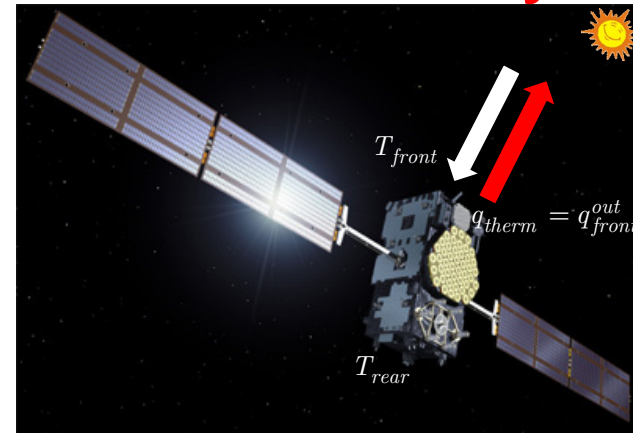
Solar Panels



absorptivity



Satellite Body



Stefan-Bolzman Law:

Thermal Flux

$$q_{therm} = q_{front}^{out} - q_{rear}^{out} = 5.67 \times 10^{-8} (\epsilon_{front} T_{front}^4 - \epsilon_{rear} T_{rear}^4) \quad [W/m^2]$$

Stefan-Boltzman constant

Acceleration induced by the thermal radiation emission

Surface temperature (front, rear)

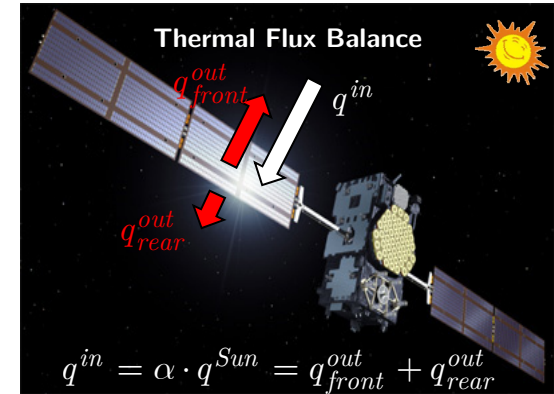
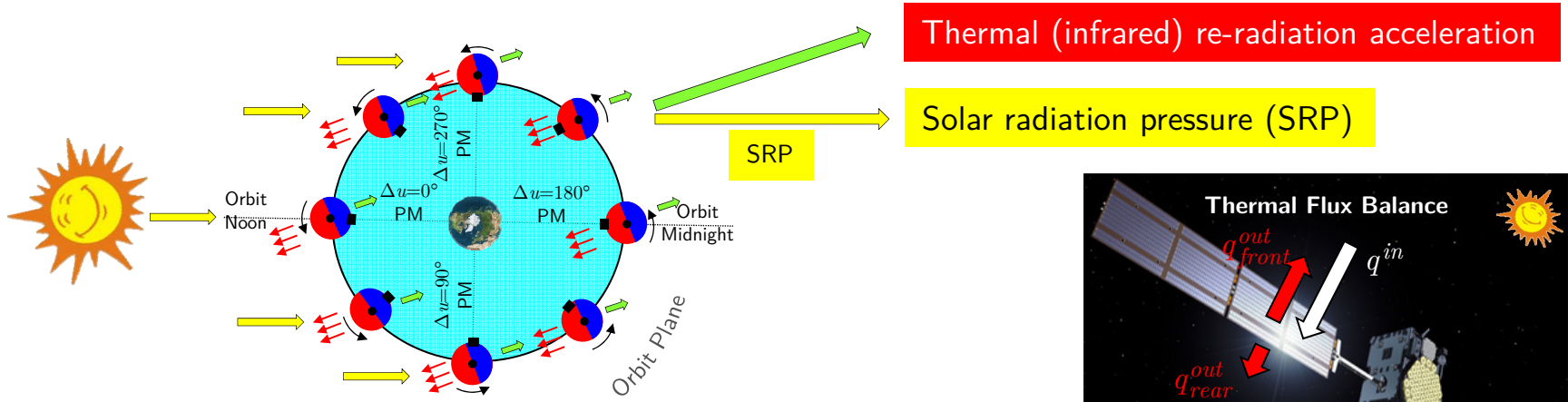
$$a_{therm} = -\frac{2}{3} C_{therm} \frac{A}{m} (\epsilon_{front} T_{front}^4 - \epsilon_{rear} T_{rear}^4) \mathbf{n}$$

$$C_{therm} = \frac{5.67 \times 10^{-8}}{c}$$

Thermal coefficient

Thermal emissivities

Thermal Re-Radiation Effect and Thermal Inertia (Yarkovsky Effect)

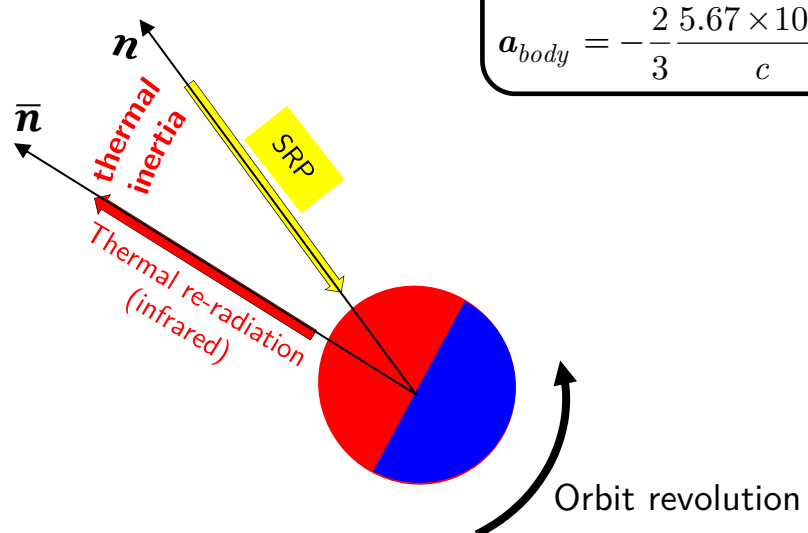
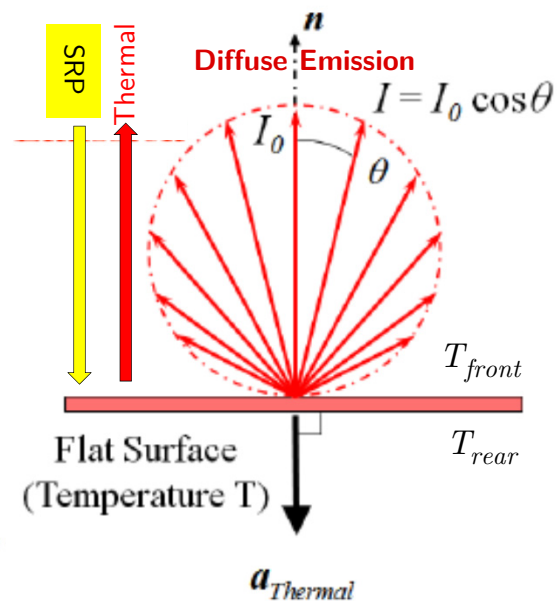


Solar Panel:

Satellite Body:

$$a_{panel} = -\frac{2}{3} \frac{5.67 \times 10^{-8}}{c} \frac{A}{m} (\epsilon_{front} T_{front}^4 - \epsilon_{rear} T_{rear}^4) \mathbf{n}$$

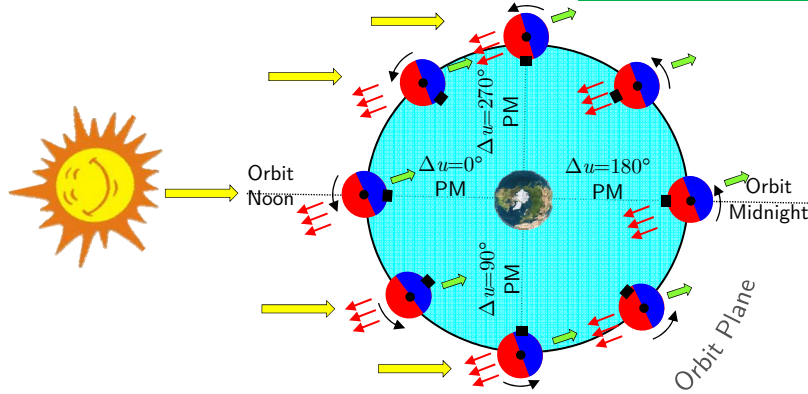
$$a_{body} = -\frac{2}{3} \frac{5.67 \times 10^{-8}}{c} \frac{A}{m} \epsilon_{body} T_{body}^4 \bar{\mathbf{n}}$$



Thermal Re-Radiation Effect and Thermal Inertia (Yarkovsky Effect)

Solar radiation (SRP)

Thermal (infrared) re-radiation acceleration



Hill Equations:

exact solution for the periodic (orbit) acceleration

$$\Delta a_i = A_i \cos nt + B_i \sin nt + C_i \quad i = \begin{cases} \text{radial} \\ \text{along} \\ \text{across} \end{cases}$$

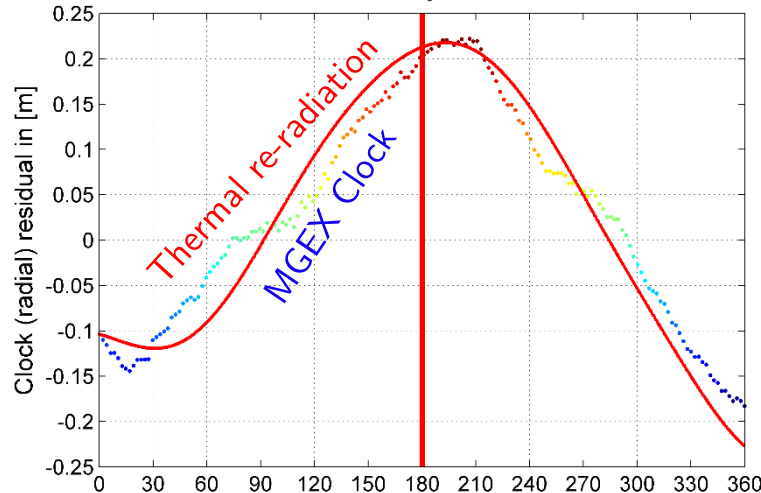


$$\Delta x_i = f(A_i, B_i, C_i, n) \quad i = \begin{cases} \text{radial} \\ \text{along} \\ \text{across} \end{cases}$$

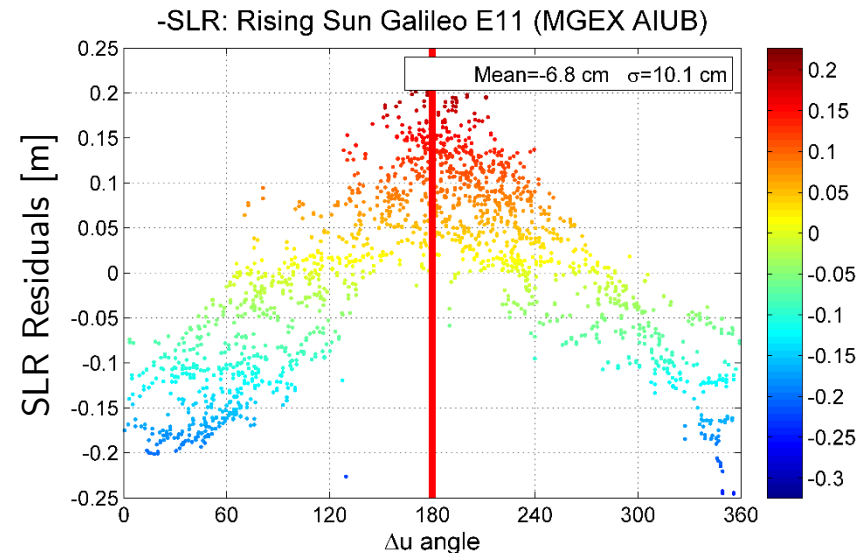
(Colombo, 1989)

Estimated thermal inertia = 4.7 min

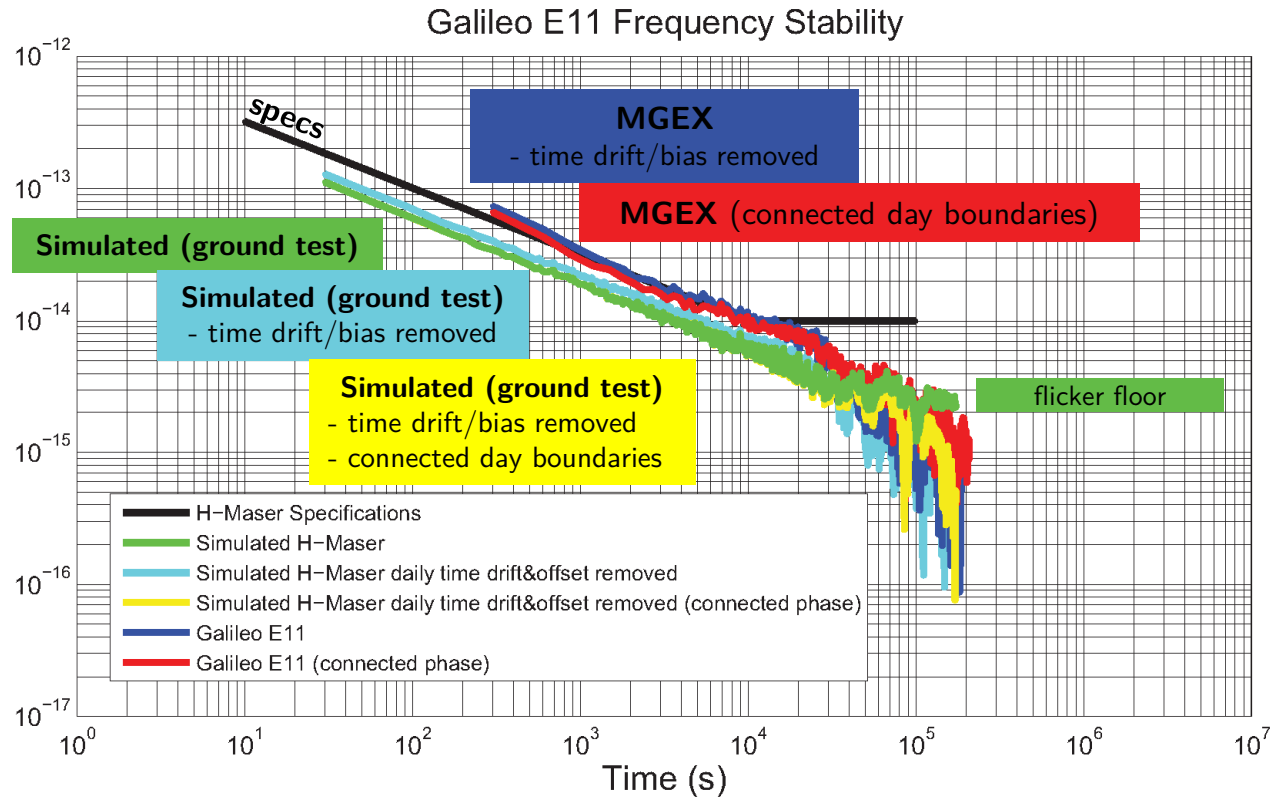
Effect of the Yarkovsky thermal re-radiation



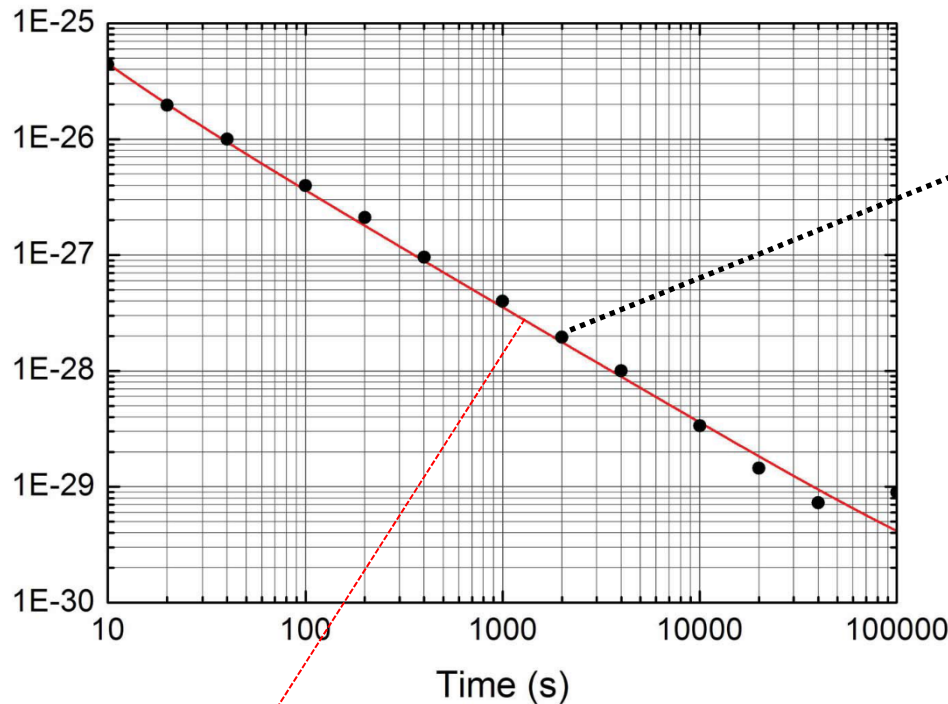
SLR Residuals (1/2 draconic year)



Allan Deviation



Clock Noise Model: Overlapping Allan Variance from the Ground Test



$$f(\tau) = \frac{A^2}{\tau^2} + \frac{B^2}{\tau} + C^2 + D^2\tau$$

Noise model function

- White phase noise: 9.8×10^{-13} short-term $\tau < 10$ s
- White frequency noise: 5.9×10^{-13} short-to-medium term
- Flicker frequency noise: 7.9×10^{-16} long-term $\tau > 6$ h
- Frequency drift: $1.2 \times 10^{-20}/\text{s}$ (from flight model test)

Clock Model: MGEX vs. Simulated

Simulated Galileo H-maser (only clock noise)

		Simulated Galileo H-Maser, (σ in mm)								
N		0.2 h	0.25 h	0.5 h	1.0 h	1.5 h	6 h	12 h	14 h	24 h
polynomial	1	1.2	1.4	2.0	2.7	3.4	6.8	9.3	11.2	15.5
	2	1.0	1.1	1.5	2.2	2.7	5.7	7.7	8.8	10.3
	3	0.8	0.9	1.3	1.9	2.3	4.7	6.5	7.8	9.8
	4	0.7	0.8	1.2	1.7	2.1	4.3	5.8	6.6	8.7
	5	0.8	0.9	1.1	1.5	1.9	3.8	5.2	5.6	7.8

Polynomial removed:

N=1 Linear model

N=2 Quadratic model

N=3

N=4

N=5

MGEX (AIUB)

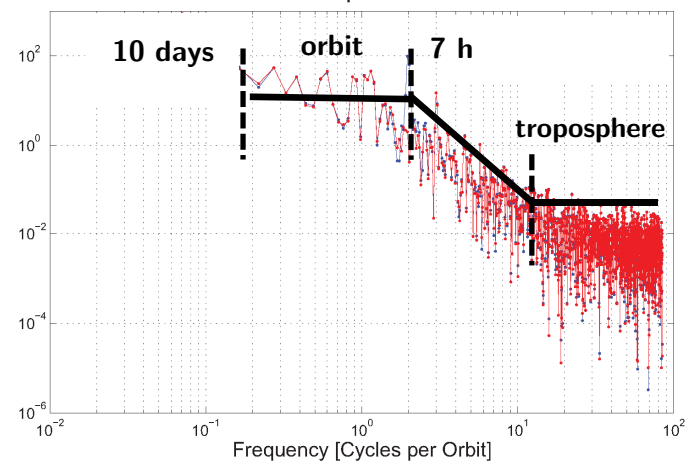
		MGEX (AIUB) Clock Parameters, (σ in mm)								
N		0.2 h	0.25 h	0.5 h	1.0 h	1.5 h	6 h	12 h	14 h	24 h
polynomial	1	-	1.8	2.9	4.2	5.3	10.9	16.2	18.3	20.2
	2	-	-	2.3	3.7	4.2	8.3	12.5	14.1	17.8
	3	-	-	1.8	3.1	3.8	7.1	10.4	12.4	16.9
	4	-	-	1.3	2.8	3.4	6.4	9.3	10.4	12.9
	5	-	-	-	2.8	3.2	5.6	8.5	9.6	11.9

$$\text{DIFFERENCE} = \sqrt{\text{MGEX}^2 - \text{SimulatedHmaser}^2}$$

		Difference MGEX-Simulated, (σ in mm)								
N		0.2 h	0.25 h	0.5 h	1.0 h	1.5 h	6 h	12 h	14 h	24 h
polynomial	1	-	1.1	2.1	3.2	4.0	8.5	13.3	14.5	13.1
	2	-	-	1.7	2.9	3.2	6.1	9.8	11.0	14.4
	3	-	-	1.2	2.4	3.0	5.3	8.1	9.7	13.8
	4	-	-	0.5	2.2	2.7	4.7	7.3	8.1	9.6
	5	-	-	-	2.3	2.6	4.2	6.7	7.9	9.0

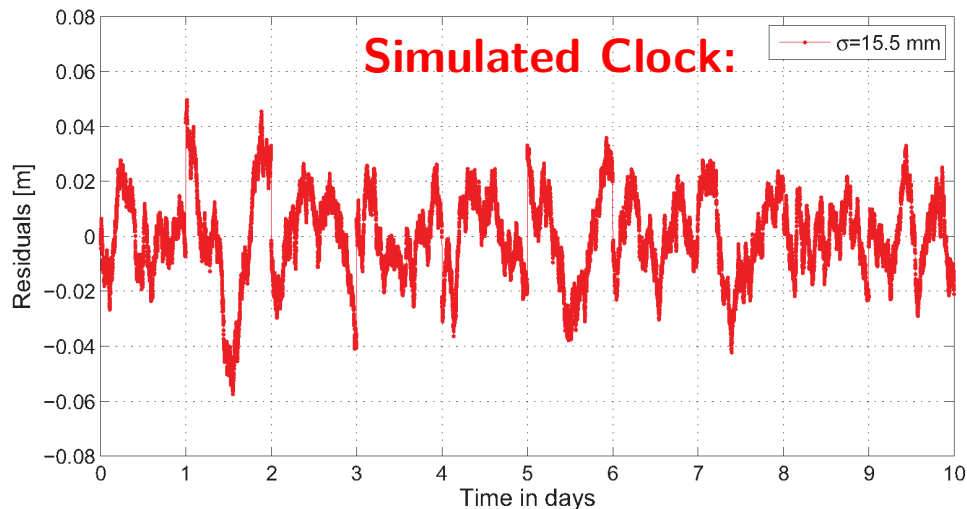
Ground network noise:

PSD of residual clock parameters 96-106/2013

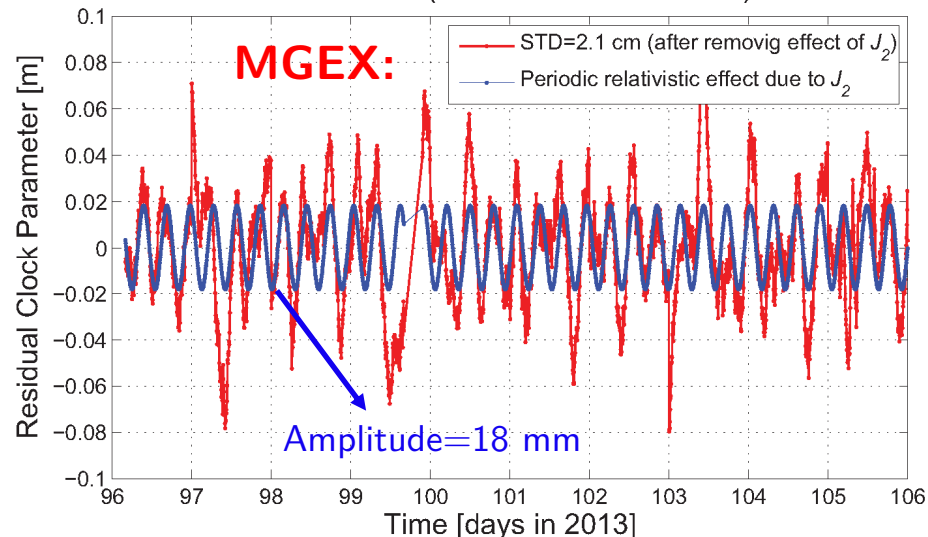


J_2 Periodic Relativistic Effect

Simulated Galileo Residual Clock Parameters



Galileo E11 (Sun Elevations 60°–65°)

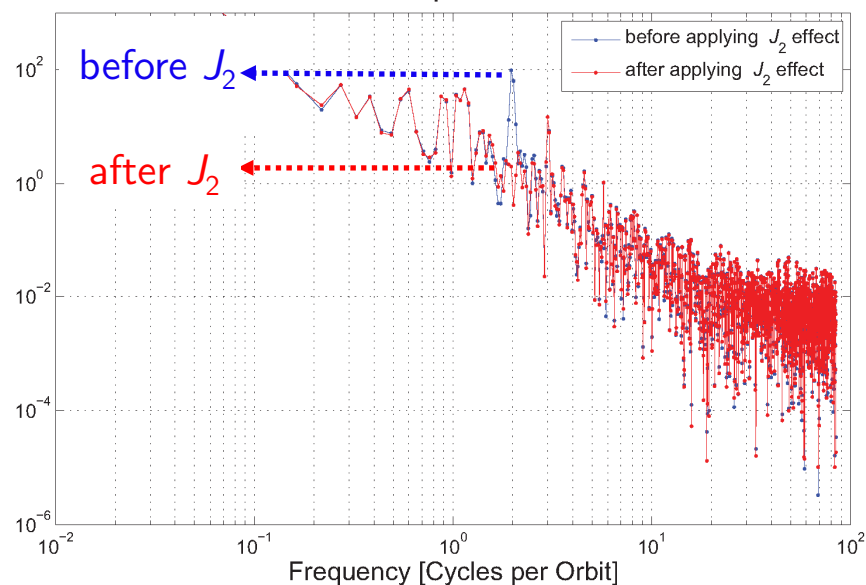


J_2 Periodic Relativistic Corrector

$$\Delta t(J_2)_{per} = -\frac{3}{2} \frac{a_e^2}{a^2 c^2} J_2 \sqrt{GMa} \cdot \sin^2 i \sin 2u$$

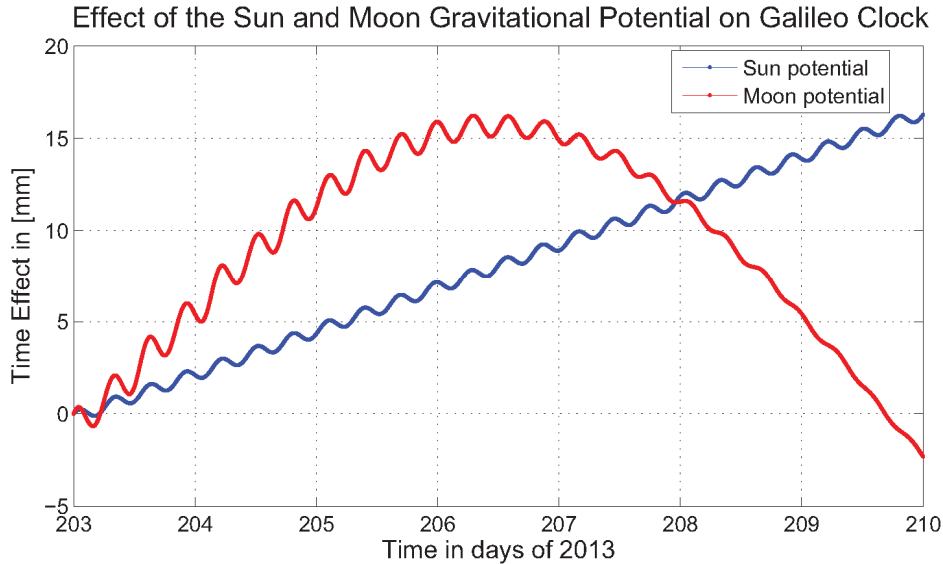
(Kouba, 2004)

PSD of residual clock parameters 96–106/2013

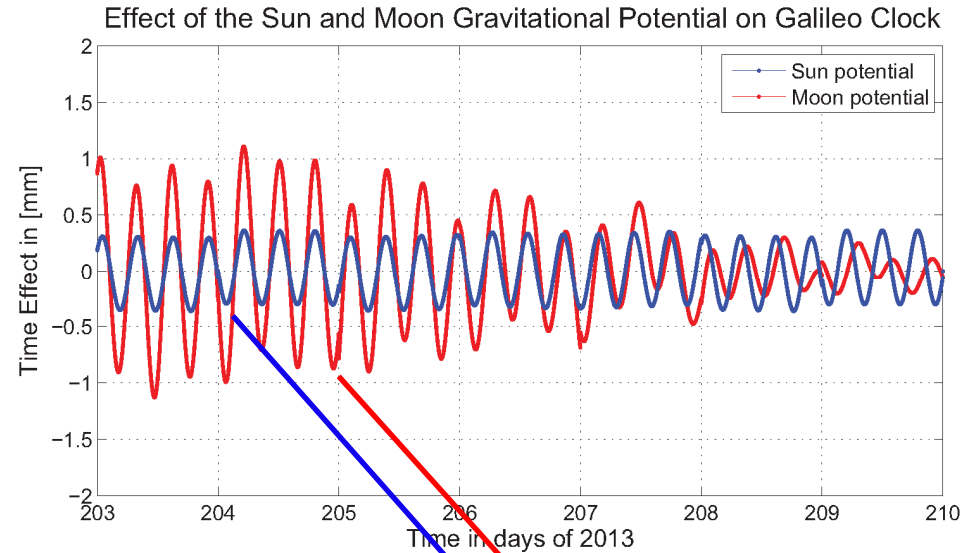


Gravitational Potential of Sun and Moon

Accumulated time over 7 days



After removing daily time drift/bias



Proper time of the clock:

$$\frac{d\tau}{dt} = 1 - \frac{1}{c^2} \left[\frac{\mathbf{v}^2}{2} + \underbrace{U_E(\mathbf{x}) + V(\mathbf{X}_A) - V(\mathbf{X}_E) - x_A^i \partial_i V(\mathbf{X}_E)} \right] \quad (\text{Petit and Luzum, 2010})$$

contribution from Sun and Moon:

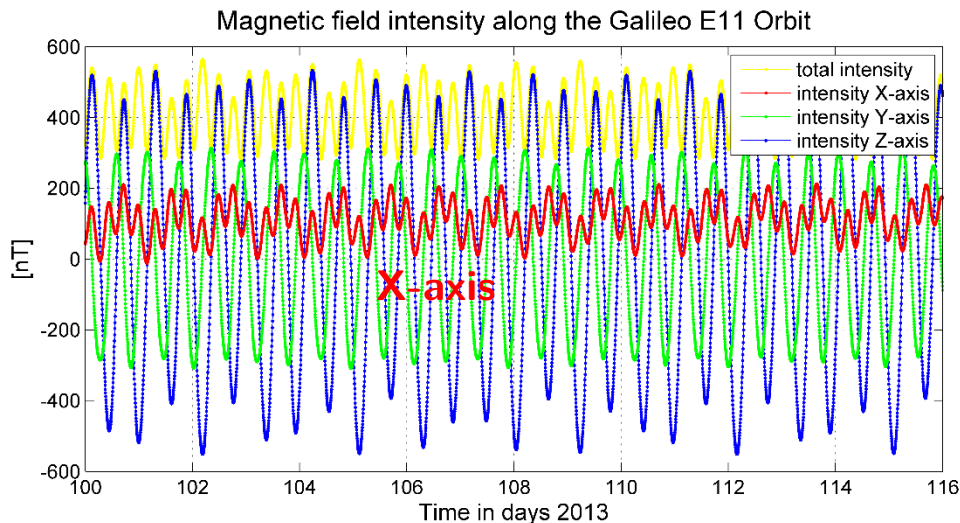
$$V(\mathbf{X}_A) - V(\mathbf{X}_E) - x_A^i \partial_i V(\mathbf{X}_E) = \sum_{A \neq E} GM_A \left[\frac{1}{r_{AP}} - \frac{1}{r_{AE}} + \frac{\mathbf{x}_{AE} \mathbf{x}_{EP}}{r_{AE}^3} \right] \quad (\text{Wolf and Petit, 1995})$$

Effect of the Earth's Magnetic Field

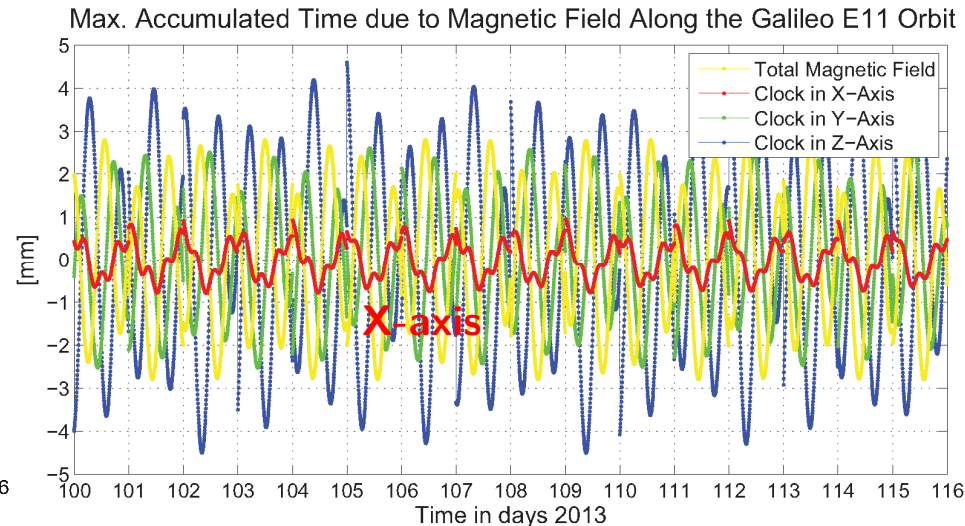
Magnetic Sensitivity:
(as measured during ground tests)

$< 3 \times 10^{-13} / \text{Gauss}$ (Boving et al., 2009)
(1 Gauss = 10^{-4}T)

IGRF model:



Linear model (time drift/bias) removed



IGRF model:

total magnetic field variation 300-550 nT

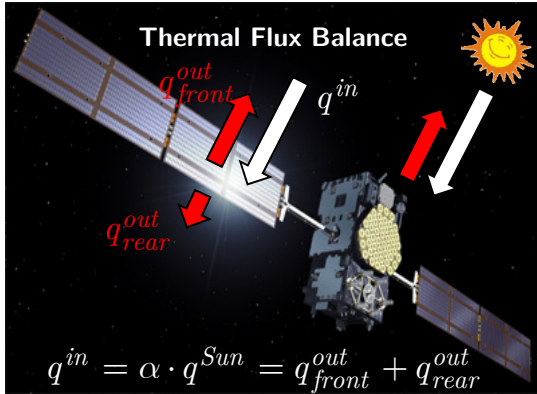


max. effect $< 0.8 \text{ mm}$

assuming the orientation of the Galileo maser cavity
along the satellite X-axis (that never faces Sun)

Thermal Sensitivity

Satellite Surface Temperature Along the Orbit:



thermal balance:

$$\alpha \cdot J_{Solar} = \varepsilon \cdot J_{re-radiated}$$

$$\alpha \cdot \frac{3.856 \times 10^{26}}{4\pi d^2} = \varepsilon \cdot 5.67 \times 10^{-8} T^4$$

Solar radiation intensity

Thermal re-radiation intensity

emittance

absorptance

$$\left. \begin{array}{l} \alpha / \varepsilon \text{ (black paint)} = 1.08 \\ \alpha / \varepsilon \text{ (kapton)} = 0.63 \end{array} \right\} \rightarrow$$

Max. temperature variation orbit noon-midnight:

$$\Delta T = 0.07^\circ C - 0.08^\circ C$$

Clock Thermal Sensitivity:

(as measured during ground tests)

$$\leq 2 \times 10^{-14} / ^\circ C \quad (\text{Boving et al., 2009})$$

(Mattioni et al., 2002)

ground platform temperature variations of 5°C

temperature stabilized within **3 m°C** (by cavity thermal control)

$$\Delta f/f \ll 10^{-15}$$

In addition:

orientation of the Galileo maser cavity is along the satellite +X-axis (that never faces the Sun)

Conclusions

- **Thermal re-radiation (and thermal inertia) can explain the distinct clock/orbit pattern over a draconic year!**
- SLR bias in Galileo (and GPS) orbits can be explained by orbit shift opposite to the Sun direction due to the thermal re-radiation of the satellite body (SRP is too small for satellite body).
- **Geometrical Mapping of Orbit Perturbations** using onboard GNSS clock is a new technique to monitor orbit errors and was successfully applied to the modelling of thermal re-radiation acceleration (thermal inertia)
- **Galileo clock (MGEX and ground test) is showing smaller standard deviation compared to SLR**
- Simulated Galileo residual clock parameters show a standard deviation of $\sigma=15.5$ mm, when time bias and time drift (linear model) is removed over 24 h intervals from the simulated epoch-wise Galileo clock parameters over 10 days, whereas this standard deviation is reduced to $\sigma=11.2$ mm when the linear model is removed every 14 h (orbit period), down to $\sigma=2.7$ mm after time bias and time drift removal on the 1 h.
- The main perturbation affecting the Galileo clock parameters for high Sun elevation ($>60^\circ$) is the the periodic relativistic effect due to J_2 gravity field coefficient (amplitude of about **18 mm**)
- Accumulated time along the Galileo orbit due to the gravitational potential of Sun and Moon after removing daily time bias and time drift shows distinct 2x per orbit effect below **0.4 mm for the Sun** and **1 mm for the Moon potential**.
- Environmental effects, such as variations in temperature and magnetic field were integrated along the orbit, but did not give a significant impact on the Galileo residual clock parameters. The max. effect of magnetic field is below **0.8 mm** whereas temperature perturbations are well below 1×10^{-15} .

Absolute Code Biases: DCBs Without TEC Maps

Differential Code Bias:

$$DCB_{P_1, P_2} := AB_1 - AB_2$$

Absolute Code Bias on P_1

Absolute Code Bias on P_2

Graphic Linear Combination:

$$LP_1 = \frac{1}{2}(P_1 + L_1) = \rho + \frac{1}{2}\lambda_1 N_1 + c\delta t - c\delta t^s + \frac{1}{2}AB_1 + \varepsilon(LP_1)$$

Iono-Free Linear Combination:

$$L_{iono-free} = \frac{f_1^2}{f_1^2 - f_2^2} L_1 - \frac{f_2^2}{f_1^2 - f_2^2} L_2 = \rho + \lambda_N N_N + \frac{1}{2}(\lambda_W - \lambda_N) N_W + c\delta t - c\delta t^s$$

Ambiguity-free condition:

$$\kappa_1^{af} \lambda_N + \kappa_2^{af} \frac{\lambda_1}{2} := 0$$

Ambiguity-Free Linear Combination:

$$AF_1 = \rho + \frac{f_1}{f_1 - f_2} AB_1 - \underbrace{\frac{c \cdot f_2}{(f_1 - f_2)^2} N_W}_{\lambda = 0.67 \text{ m}} + c\delta t - c\delta t^s$$

IGS Clock Convention ("Iono-Free Clocks" based on P_1 and P_2)

Geometry-Free:

$$AF_1 - P_{iono-free} = \kappa_1^{af} L_{iono-free} + \kappa_2^{af} LP_1 - P_{iono-free} = \frac{\kappa_2^{af}}{2} AB_1$$

Absolute Code Biases with Third Frequency

$$\begin{aligned}
 L_{iono-free}^{1,2} &= \frac{f_1^2}{f_1^2 - f_2^2} L_1 - \frac{f_2^2}{f_1^2 - f_2^2} L_2 = \rho + \lambda_N N_1 + \frac{1}{2} (\lambda_W - \lambda_N) N_W \\
 L_{iono-free}^{2,5} &= \frac{f_1^2}{f_1^2 - f_2^2} L_1 - \frac{f_2^2}{f_1^2 - f_2^2} L_2 = \rho + \lambda_{N(2,5)} N_1 - \lambda_{N(2,5)} N_W + \frac{1}{2} (\lambda_{W(2,5)} - \lambda_{N(2,5)}) N_{W(2,5)}
 \end{aligned}$$

Iono-Free
Linear Combinations:

Ambiguity-free condition:

$$\kappa_1^{af*} \lambda_N + \kappa_2^{af*} \lambda_{N(2,5)} := 0$$

$$\begin{aligned}
 L_{iono-free}^{af*} &:= \kappa_1^{af*} L_{iono-free}^{1,2} + \kappa_2^{af*} L_{iono-free}^{2,5} \\
 &:= \rho + \left[\frac{\kappa_1^{af*}}{2} (\lambda_W - \lambda_N) - \kappa_2^{af*} \lambda_{N(2,5)} \right] N_W + \frac{\kappa_2^{af*}}{2} (\lambda_{W(2,5)} - \lambda_{N(2,5)}) N_{W(2,5)}
 \end{aligned}$$

Ambiguity-free condition:

$$-\frac{c \cdot f_2}{(f_1 - f_2)^2} \kappa_1^{af**} + \kappa_2^{af**} \lambda_W^{af*} := 0$$

$$AF_1 = \rho - \frac{c \cdot f_2}{(f_1 - f_2)^2} N_W + \frac{f_1}{f_1 - f_2} AB_1 + c\delta t - c\delta t^s$$

Two-frequency Ambiguity-Free LC
(previous slide)

Ambiguity-Free Linear Combination:

Geometry-Free:

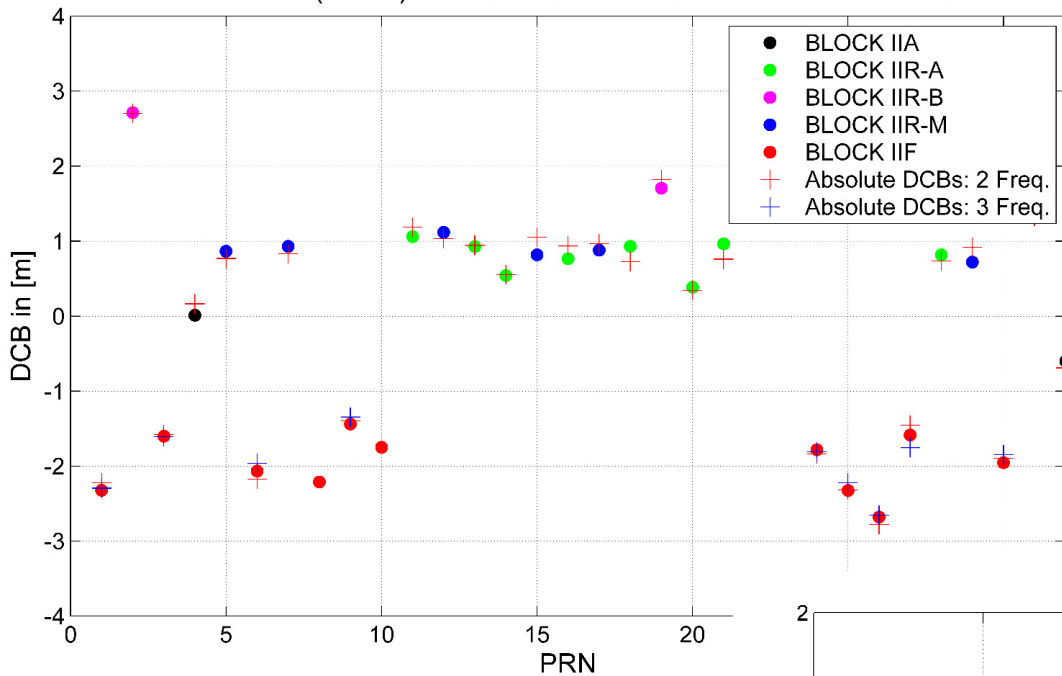
$$AB_1 = \frac{f_1 - f_2}{\kappa_1^{af**} f_1} \left[\left(\kappa_1^{af**} AF_1 + \kappa_2^{af**} L_3^{af*} - P_{iono-free} \right) - \underbrace{\kappa_2^{af**} \lambda_{W(2,5)}^{af*}}_{\lambda = 3.41 \text{ m}} N_{W(2,5)} \right]$$

$$\lambda = 3.41 \text{ m}$$

IGS Clock Convention ("Iono-Free Clocks")

CODE DCBs vs. DCBs Based on the Absolute Code Biases

CODE DCB(P1-P2) vs. DCBs Based on the Absolute Code Biases



DCB(P1-P2) - mean(per BLOCK)

